Journal of Zhejiang University-SCIENCE B (Biomedicine & Biotechnology) in press
www.jzus.zju.edu.cn; www.springer.com/journal/11585
E-mail: jzus_b@zju.edu.cn

Research Article

https://doi.org/10.1631/jzus.B2500281

MDM2/X mediate reduced apoptosis in plateau zokor: a mechanism of high-altitude adaptation

Mengchen ZHANG[1,2], Yi LI[1,2], Huiqi LIN[3], Tianfu YU[1,2], Fangyuan XIA[1,2], Mahanand CHATOO[1,2], Kexin LI[4], Honghao YU[5], Eviatar NEVO[6], Jizeng DU[2], Yang ZHAO[3]✉, Xuequn CHEN[1,2]✉

[1]*Department of Neurology of The Second Affiliated Hospital, School of Brain Science and Brain Medicine, Zhejiang University School of Medicine, Hangzhou 310016, China*
[2]*NHC and CAMS Key Laboratory of Medical Neurobiology, Zhejiang University School of Medicine, Hangzhou 310058, China*
[3]*Department of Physiology and Department of Hepatobiliary and Pancreatic Surgery of The First Affiliated Hospital, Zhejiang University School of Medicine, Hangzhou 310058, China*
[4]*State Key Laboratory of Herbage Improvement and Grassland Agro-ecosystems, College of Ecology, Lanzhou University, Lanzhou 730000, China*
[5]*College of Biotechnology, Guilin Medical University, Guilin 541004, China*
[6]*Institute of Evolution, University of Haifa, Haifa 31905, Israel*

Abstract: MDM2 (Murine double minute 2) and MDMX (Murine double minute 4) are critical for the regulation of p53 function and apoptosis. This study compares the *Mdm2/x* gene sequences and functional variations of subterranean zokors in high plateaus and loess plateaus. The findings reveal the molecular mechanisms behind how these species' MDM2/X variations drive adaptation to extremely high-altitude conditions, including low oxygen, cold temperatures, and perpetual darkness in underground environments. We cloned and analyzed *Mdm2/x* sequences from two distinct ecological groups of subterranean rodents, *Myospalax baileyi* (*M.b*., plateau zokor) and *Myospalax cansus* (*M.c*., Gansu zokor), and reconstructed phylogenetic trees for a series of rodents and mammals of subterranean species and the aboveground lab rat, as well as humans. We found that MDM2/X of *M.b*. and *M.c*. are involved in the low apoptosis rate dependent on p53, and the variations of phosphorylation sites in the C-terminal of MDM2 contribute to upregulation of p53 transcription and protein expression. We propose that gene evolutionary mechanisms enable survival under these severe combined pressures, and believe that our findings provide critical insight into how genetic modifications drive physiological resilience in Earth's most challenging ecosystems.

Key words: MDM2; Plateau zokor; Apoptosis; Adaptation; Extreme environment

1 Introduction

The function of tumor suppressor p53 is tightly regulated to avoid excessive cell death, which is largely conferred by its target gene MDM2 (HDM2 in humans, chromosome 12q15). MDM2 is an E3 ubiquitin ligase that inhibits p53 through proteasomal degradation, forming a critical negative feedback loop. Its structural homolog, MDMX (MDM4, chromosome 1q32), also suppresses p53, but lacks ubiquitin ligase activity; instead, it sterically blocks p53's transcriptional activity and stabilizes MDM2 by forming MDM2-MDMX heterodimers to exacerbate p53 degradation (Levine, 2020; Chibaya et al., 2021). In addition to the canonical roles of

✉ Xuequn CHEN, chewyg@zju.edu.cn
Yang ZHAO, yang.zhao@zju.edu.cn
Xuequn CHEN, https://orcid.org/0000-0002-6105-8869
Yang ZHAO, https://orcid.org/0000-0002-8703-3678

Received May 27, 2025; Revision accepted Sept. 10, 2025;
Crosschecked xxx. xx, 20xx; Published online xxx. xx, 20xx

MDM2/X-p53 signaling in cancers, dysregulation of this pathway is implicated in chronic pathologies, including inflammation, autoimmune disorders, and neurodegeneration (Brummer and Zeiser, 2024; Efe et al., 2024). Consequently, disruption of MDM2/X with small-molecule inhibitors has emerged as a therapeutic strategy to reactivate p53 (Chandramohan et al., 2024; Wang et al., 2024).

Survival of the fittest is starkly evident in the high-altitude plateau fauna of China. Facing relentless hypoxia, cold, and solar radiation, species like zokors have evolved robust physiological and genetic adaptations through long-term natural selection (Wei et al., 2006; Chen et al., 2007; Zhang ST et al., 2013; Zhao et al., 2013; Zhang T et al., 2022). These extreme-environment species serve as excellent models for decoding adaptive evolution, from whole-organism resilience to adaptive molecular modifications (Liu et al., 2022; Zhang T et al., 2022; Hu et al., 2023; Yu and Zhang, 2023; Zhang XY et al., 2023; An et al., 2024; Wei et al., 2025).

Two subterranean zokor species, *Myospalax baileyi* (*M.b*., syn. *Eospalax baileyi*) and *Myospalax cansus* (*M.c*., syn. *Eospalax cansus*), inhabit distinct high-altitude subterranean environments with divergent selective pressures. *M.b*. thrives in the alpine meadow (altitude around 3800 m), characterized by extreme hypoxia, intense solar particle radiation, cold temperatures, and unique geological soil composition (acidity and metal cation content). In contrast, *M.c*. occupies the loess plateau (altitude around 800 m), and is exposed to distinct challenges: high CO_2 levels in burrows and drier soils. These environmental disparities likely drive species-specific physiological and genetic adaptations, particularly in terms of hypoxia response, metabolism, and stress-resistance pathways (Wei et al., 2006; Chen et al., 2007; Deng et al., 2014; Shao et al., 2015; Cai et al., 2018; Gao et al., 2023; An et al., 2024). Previous studies have identified adaptive mechanisms in subterranean species (*M.b*. in China and blind mole rat in Israel), including modifications in p53, HIFs (hypoxia-inducible factors), and IGF (insulin-like growth factor) pathways (Chen et al., 2007; Zhang et al., 2013; Zhao et al., 2013; Zhao et al., 2016).

In this study, we investigate the transcriptional regulation of MDM2 and MDMX in *M.b*. and *M.c.* in their extreme subterranean habitats. We cloned and analyzed *Mdm2/x* sequences from these subterranean rodents and compared them with those of aboveground species. Our findings demonstrate that *M.b*./*M.c*.-MDM2/X inhibit apoptosis in a p53-dependent manner, with phosphorylation variations in the C-terminal of MDM2 playing a critical role in regulating p53 accumulation. These results reveal how species-specific MDM2/X variants drive adaptation to extreme hypoxic conditions, particularly through suppression of apoptosis. We propose that evolutionary modifications in these genes underlie the remarkable physiological resilience of subterranean rodents, enabling survival under combined stressors, particularly hypoxia.

2 Materials and methods

2.1 Animals and hypoxia treatment

Myospalax baileyi (240-280 g) were captured around Haibei Research Station of the Alpine Meadow Ecosystem, Chinese Academy of Sciences, in Qinghai, China (equivalent to 11.0%-13.0% O_2 at sea level, 37°39′N, 101°19′E, altitude 3000-4500 m). *Myospalax cansus* (180-240 g) were captured in Yulin, northern Shaanxi (37°06′N, 107°15′E, altitude about 800 m). As both species complete their life cycle in subterranean burrows (70-250 cm depth) characterized by hypoxia and hypercapnic conditions (Zeng et al., 1984; Tian et al., 2017), a comparative study was conducted. *Rhizomys pruinosus* (*R.p*., bamboo rat, 290-350 g) were obtained from Yangshuo, northeastern Guangxi, China (24°53′N, 110°20′E, altitude 300 m). Adult male Sprague–Dawley rats (180-200 g; certification No. SCXK20190002) were purchased from the Laboratory Animal Center of Zhejiang Academy of Medical Sciences. All animals were housed under controlled environmental conditions (21-23 °C, 12 h light/dark cycle) with free access to food and water.

For hypoxia treatment, the lab rats underwent hypobaric hypoxia exposure (10.8% or 8.0% O_2 for 8 h) in a hypobaric chamber (FLYDWC50-IIC; Avic Guizhou Fenglei Aviation Armament Co., Ltd.) to mimic altitudes of 5000 m and 7000 m, respectively (Zhao et al., 2013). Lung, spleen, and liver tissues were immediately cryopreserved in liquid nitrogen and subsequently stored at -80 °C.

2.2 Cloning of *Mdm2* and *Mdmx* from *M. baileyi*, *M. cansus*, and *R. pruinosus*

The *Mdm2* and *Mdmx* cDNA of *M.b.* (GenBank accession No. KR149455.1 and MH033626), *M.c.* (KR149456.1 and MH033627), and *R.p.* (PV700090 and PV700091) were cloned in our lab. Primers were designed based on various *Mdm2* and *Mdmx* sequences in GenBank: rat (XM_006241383.2 and NM_001012026.1), blind mole rat (*Nannospalax galili*, *N.g.*, syn. *Spalax galili*, *S.g.*) No. XM_017801625.2 and XP_008828611.1, and human (BT007935.1 and AF007111.1). To confirm the authenticity of each varied codon, we cloned genes from the lung and liver tissues of six individuals of each species.

2.3 Multiple alignments, phylogenetic tree, and 3D structure analysis

The sequence alignments of MDM2, MDMX, and p53 proteins in *M.b.*, *M.c.*, *R.p.*, and 13 other species were generated using Multalin software (http://multalin.toulouse.inra.fr/multalin). The phylogenetic trees were constructed with ClustalW and MEGA7 software based on the amino acid sequences, using the neighbor-joining method (Zhao et al., 2023). The accession numbers of MDMX, MDMX, and p53 genes in the phylogenetic trees are listed in Table S1. We predicted the 3D structures (MDM2, MDMX, p53, and p53-MDM2 complex) using AlphaFold 3 (https://alphafoldserver.com/) and displayed them with PyMOL.

2.4 Cell cultures and hypoxia treatment

The cell lines H1299 (human non-small-cell lung cancer) and HEK293T (human embryonic kidney 293 cells) were grown in medium RPMI 1640 (Gibco) or DMEM (Gibco), respectively, containing 10% (v/v) FBS (Gibco), 100 μg/mL streptomycin (Solarbio), and 100 U/mL penicillin (Solarbio), at 37 °C in a humidified incubator with 5% (v/v) CO_2.

The hypoxia treatment for cells was performed using the hypoxia controller (BioSpherix). The cell medium was replaced at 12 h posttransfection before cells were moved to the hypoxia chamber (0.1% O_2, 24 h).

2.5 Quantitative real-time RT-PCR

The *Mdm2*, *Mdmx*, and *p53* mRNA quantities were determined by real-time RT-PCR. Primers were synthesized according to the gene sequences of rat, *M.b.*, and *M.c.* as follows:
rat *Mdm2*-F: 5′-AGG ATG ATG AGG TCT ATC GGG T-3′;
rat *Mdm2*-R: 5′-AAG CCA GTT CTC ACG AAG GG-3′;
M.b. Mdm2-F: 5′-GCA AGA GCC ACA GGA AGA GA-3′;
M.b. Mdm2-R: 5′-GTG GCG CTT TCT TTG TCG TT-3′;
M.c. Mdm2-F: 5′-TCT GGT GAT TGG TTG GAT CAA GA-3′;
M.c. Mdm2-R: 5′-TCT GCA TCA CTT TCC CCT GC-3′;
Mdmx-F: 5′-CAA GAC CGA CTG AAG CAC GG-3′;
Mdmx-R: 5′-CAG CAA CAT CCC ACT CCT CAA-3′;
rat *p53*-F: 5′-GTG CAC GTA CTC AAT TTC CCT C-3′;
rat *p53*-R: 5′-TCA GAG CAA CGC TCA TGG TG-3′;
M.b. p53-F: 5′-GAG CGC TGC TCTGAT AGT GA-3′;
M.b. p53-R: 5′-TGC CTC CCA TAC AGG AGC TAT-3′;
M.c. p53-F: 5′-GGC TCT GAC TGT ACC ACC AT-3′;
M.c. p53-R: 5′-AGG CAC AAA CTC GAA CCT CA-3′;
β-actin-F: 5′-AGC CAT GTA CGT AGC CAT CC-3′;

β-actin-R: 5′-CTC TCA GCT GTG GTG GTG AA-3′.

2.6 Western blotting

Western blotting was performed to determine the MDM2, MDMX, and p53 protein levels in the tissues and cells under hypoxia. Samples were lysed in 300 μL RIPA Lysis Buffer (Solarbio) with 1 mM PMSF (Solarbio). The extracts were centrifuged at 12000 g for 15 min (4 °C), then mixed with loading buffer and boiled at 95 °C for 5 min. Protein samples were subjected to electrophoresis, then transferred to the PVDF membrane, and incubated overnight with target protein primary antibodies (MDM2: SPM344, Invitrogen; MDMX: MDMX-82, Abcam; p53: 1C12, Cell Signaling; GFP-tag: Yeasen; β-actin: Yeasen). The second antibodies were incubated at room temperature for 1 h before the samples were visualized with ECL.

2.7 Plasmids

For p53-expression plasmids, the coding regions of rat, *M.b.*, and *M.c.* sequences were ligated into the pEGFP-N1 expression vector. The wild-type MDM2, MDMX of rat, *M.b.*, and *M.c.*, and mutant MDM2-F390Y (TAT substitute TTT to change the amino acid), MDM2-A415T (ACA to GCC) plasmids of *M.b.* and *M.c.* were ligated into the pcDNA3.1+ expression vector. All fragments ligated into the vectors were sequenced to confirm authenticity.

2.8 Transient transfection

H1299 and HEK293T cells were plated in 6-well plates for 18 h, then the medium was replaced with a complete medium of serum and antibiotics 30 min before transfection. Transient transfection was performed using PolyJet transfection reagent (SignaGen). Cells were co-transfected with a mixture of MDM2, MDMX, or p53 expression plasmids. The PolyJet/DNA complex-containing medium was replaced with fresh complete serum/antibiotics-containing medium 12 h posttransfection, and the cells were transferred to the hypoxia chamber. Cells were harvested 48 h posttransfection.

2.9 Flow Cytometry

For cell apoptosis, H1299 and HEK293T cells were transfected with the indicated plasmids. After 48 h of transfection and hypoxia treatment, cells were cleaned with cold PBS and collected. Cells were resuspended in binding buffer, then stained with Annexin V-phycoerythrin (PE) and 7-amino-actinomycin D (7-AAD) for 15 min at room temperature, and cells were analyzed using flow cytometry. Samples were gated to GFP-positive cells to confirm that all the analyzed cells expressed the transfected p53. The p53-induced apoptosis rate was calculated as the percentage of PE^+ with $7\text{-}AAD^-$ cells.

2.10 Statistical Analysis

Statistical analysis was conducted using GraphPad Prism 8 software. The statistical significance compared with the control was determined using a two-tailed, unpaired Student's t-test. Comparisons between multiple groups were conducted using one-way ANOVA, followed by the Tukey test.

3 Results

3.1 Comparison and phylogenetic trees of *M.b.* and *M.c.* MDM2 and MDMX sequences

The *Mdm2* and *Mdmx* mRNAs of the subterranean *M.b.* (Tibet plateau), *M.c.* (Loess plateau) and *R.p.* (bamboo forest) were cloned and sequenced. The coding regions of *M.b.*, *M.c.*, and *R.p.* MDM2 are composed of 1467bp (coding a protein of 488aa, KR149455.1), 1464bp (487aa, KR149456.1), and 1464bp (487aa,

PV700090). The coding regions (CDS) of *M.b.*, *M.c.*, and *R.p.* MDMX are composed of 1473bp (490aa, MH033626), 1473bp (490aa, MH033627), and 1476bp (491aa, PV700091). In addition, we also cloned and sequenced *R.p.*-p53 (1164 bp, 388 aa, PV700089) for reconstructing phylogenetic trees.

M.b. and *M.c.* MDM2 proteins have 99.40% identity, and both have identities of 91.00% and 90.40%, 84.80% and 84.20%, 95.70% and 95,00%, 92.60% and 92.60% with humans, rats, *N.g.*, and *R.p.* MDM2 protein, respectively. *M.b.* and *M.c.* MDMX proteins have 85.70% identity, and both have identities of 82.30% and 84.80%, 82.90% and 85.40%, 84.7%, and 87.90%, 88.90% and 87.80% with humans, rats, *N.g.*, and *R.p.* MDMX protein, respectively. Phylogenetic trees based on the MDM2, MDMX, and p53 sequences are similar, indicating that *M.b.*, *M.c.*, *R.p.*, and *N.g.* of subterranean rodents evolved adaptively and convergently against hypoxia and a high CO_2 environment (Fig. 1a).

Multiple alignment analysis was performed using Multalin software as described (Corpet F, 1988). Both MDM2 and MDMX contain the p53 binding domain, Acidic domain, Zinc domain, and RING domain. The domain sequences of MDM2, MDMX, and p53 are conserved across species (Fig. S1-S3). The variations are widely distributed across coding regions at *M.b.*, *M.c.*, *N.g.*, and *R.p.* or *M.o.* and *M.och.* (Fig. 1b). Some variations presented in MDM2 coding regions of *M.b.*, *M.c.*, and *R.p.*, such as T62S of *R.p.* in the p53 binding domain, unique R126K of *R.p.*, and G131S of *R.p.* and *M.c.*. There are some variations around acidic and zinc domains (codons 211, 212, 331). Interestingly, we found two specific variations, A/V415 (T in humans and rats) and F390 (Y in humans and rats), in *M.b.*, *M.c.*, *R.p.*, and *N.g.* between the Zinc and RING domains. These sites are involved in the classical ATM-induced MDM2 activation. There are some variations in the MDMX coding region, including T145S and A178T of *M.b.*, *M.c.*, and *R.p.*; codon 151 deletion and V225A of *M.b.* and *M.c.* (close to acidic domain), and the unique K273R mutation of *M.b.* and *M.c.* between acidic and zinc domains (*vs* humans). Therefore, MDM2 and MDMX share conserved domains throughout evolution, the common variations among *M.b.*, *M.c.*, and *R.p.* mainly in non-domain regions.

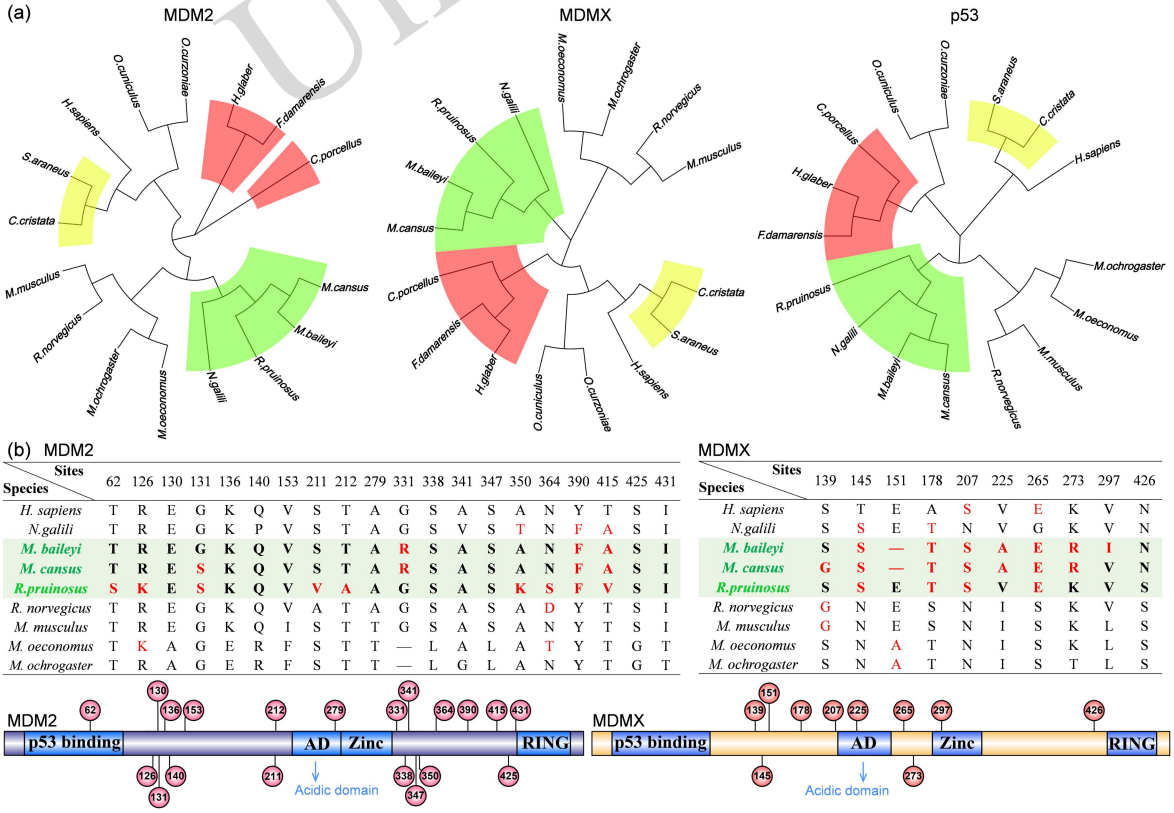

Fig. 1 Comparative analysis of MDM2, MDMX, and p53 gene evolution in subterranean species. (a) Phylogenetic trees

based on MDM2, MDMX, and p53 protein sequences of *M.b.*, *M.c.*, and *R.p.*, as well as those of other subterranean animals using the neighbor-joining method (16 species). *Spalacidae* in green, *Hystricomorpha* in red, and *Insectivora* in yellow. (b) Multiple alignments and variation sites of MDM2, MDMX, and p53 amino acid sequences. The diagrams below show the domain structures of MDM2 and MDMX, corresponding variation codons in *M.b.*, *M.c.*, and *R.p.*.

3.2 High *Mdm2* and *p53* mRNA expression in lung, liver, and spleen of *M.b.* and *M.c.*

We compared the basal transcriptional levels of *Mdm2* and *Mdmx* in different tissues of subterranean zokors and aboveground lab rats with hypoxia exposure. The qPCR analysis revealed high expression of *Mdm2* in the lung, liver, and spleen of *M.b.* and *M.c.* (Fig. 2a), while *Mdmx* was notably elevated only in *M.c.* lung. However, hypoxia-exposed lowland lab rats showed decreased *Mdmx* mRNA in the liver and increased *Mdm2* mRNA in the spleen (Fig. 2b). In Addition, enhanced *p53* mRNA in *M.b.* and *M.c.* tissues are the same as *Mdm2* mRNA (Fig. 2c), whereas hypoxic rats exhibited opposing tissue-specific responses: downregulated in the lung and upregulated in the spleen. These results suggest a unique co-upregulation of *Mdm2* and *p53* in subterranean rodent tissues, distinct from hypoxia-induced shifts in rats (Fig. 2d), potentially reflecting adaptive mechanisms to their subterranean environment.

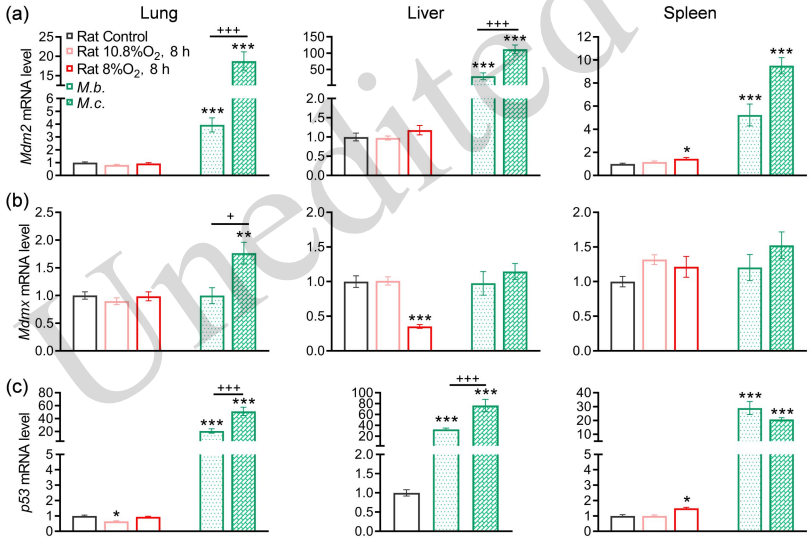

(d)

tissue \ gene	*Mdm2*	*Mdmx*	*p53*	Animal	Stress
Lung	—	—	—	Rat	Control, 21% O_2
	—	—	↓		10.8% O_2, 8 h
	—	—	—		8% O_2, 8 h
	↑↑↑	—	↑↑↑	*M.b.*	
	↑↑↑	↑↑	↑↑↑	*M.c.*	
Liver	—	—	—	Rat	Control, 21% O_2
	—	—	NA		10.8% O_2, 8 h
	—	↓↓↓	NA		8% O_2, 8 h
	↑↑↑	—	↑↑↑	*M.b.*	
	↑↑↑	—	↑↑↑	*M.c.*	
Spleen	—	—	—	Rat	Control, 21% O_2
	—	—	—		10.8% O_2, 8 h
	↑	—	↑		8% O_2, 8 h
	↑↑↑	—	↑↑↑	*M.b.*	
	↑↑↑	—	↑↑↑	*M.c.*	

Fig. 2 The lung, liver, and spleen of *M.b.* and *M.c.* contain higher levels of *Mdm2* and *p53* mRNA expression. Comparison analysis of *Mdm2* (a), *Mdmx* (b), and *p53* (c) transcription in *M.b.*, *M.c.*, and lab rats under hypoxia challenge. Values are given as mean±SEM, n=6, $^{*}P<0.05$, $^{**}P<0.01$, $^{***}P<0.001$ (*vs* rat control), $^{+}P<0.05$, $^{+++}P<0.001$ (*vs M.c*). (d) Summarized data of subterranean rodents showed a significant upregulation compared to lab rats under hypoxia. ↑, up-regulation; ↓, down-regulation; −, unchanged; NA, not available (published data).

3.3 High MDM2, MDMX, and p53 protein expression in the lung and liver of zokors

As we demonstrated above, the mRNA abundance of *Mdm2*, *Mdmx*, and *p53* in the subterranean zokors

differs across tissues, we next examined the protein functions. Protein expression analysis demonstrated the elevated MDM2, MDMX, and p53 in both lung and liver tissues of *M.b.* and *M.c.* (Fig. 3a and 3b), with high MDMX expression specifically in *M.b.*-spleen (Fig. 3c). In lowland lab rats subjected to hypoxia, we found increased MDM2, MDMX, and p53 protein levels in the lung tissue, along with enhanced p53 (but not MDM2 or MDMX) in the liver, a finding consistent with our previous reports (Zhao et al., 2013). Notably, these hypoxia-induced changes were absent in spleen tissue (Fig. 3c). This tissue- and species-specific pattern suggests different regulatory mechanisms between constitutively adapted subterranean rodents and acute hypoxia-challenged rats.

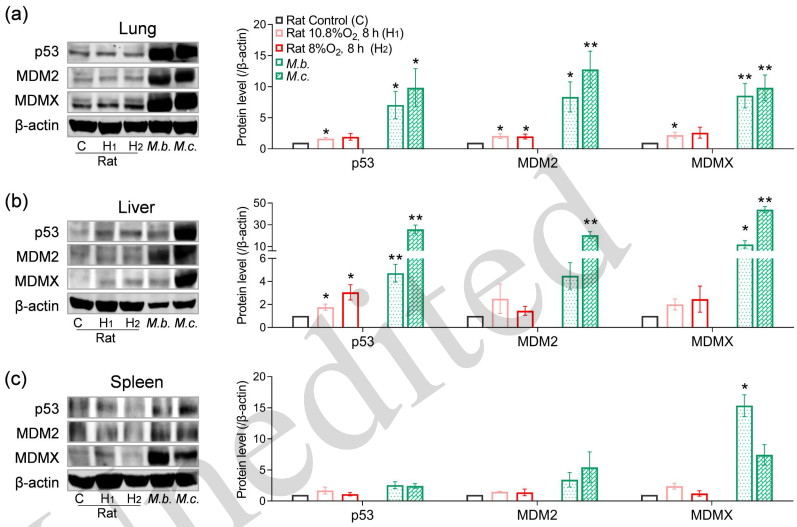

Fig. 3 Subterranean zokors showed high p53, MDM2, and MDMX protein levels in the lung. Western blotting showing protein expression in the lung (a), liver (b), and spleen (c) in *M.b.*, *M.c.*, and rats under hypoxic stress (H1: 10.8% O_2, H2: 8% O_2). Values are given as mean±SEM, n=6, $^{*}P < 0.05$, $^{**}P < 0.01$ (*vs* rat control).

3.4 MDM2/X induces lower p53-dependent apoptosis in subterranean zokor

To elucidate the regulatory role of *M.b.* and *M.c.*-MDM2/X in p53-mediated apoptosis, we conducted gain-of-function experiments in p53-null H1299 cells. Co-expression of rats or *M.c.*-p53 with their respective MDM2/MDMX (individually or combined) significantly enhanced apoptosis (Fig. 4a and 4c), but this p53-induced increase was not observed in *M.b.* (Fig. 4b and 4d). Under hypoxia, the apoptosis of subterranean groups was generally lower and was further down-regulated by *M.b.*-MDM2/X and *M.c.*-MDM2 (Fig. 4d). A similar phenotype was consistently observed in HEK293T cells, MDM2/X-p53 in *M.b.* and *M.c.* showed lower apoptosis rates both in normoxia and hypoxia (Fig. 4e). These findings demonstrate that *M.b.*/*M.c.*-MDM2/X exhibit a protective anti-apoptotic function in the p53-mediated apoptosis (independent of cell types), particularly under hypoxic conditions.

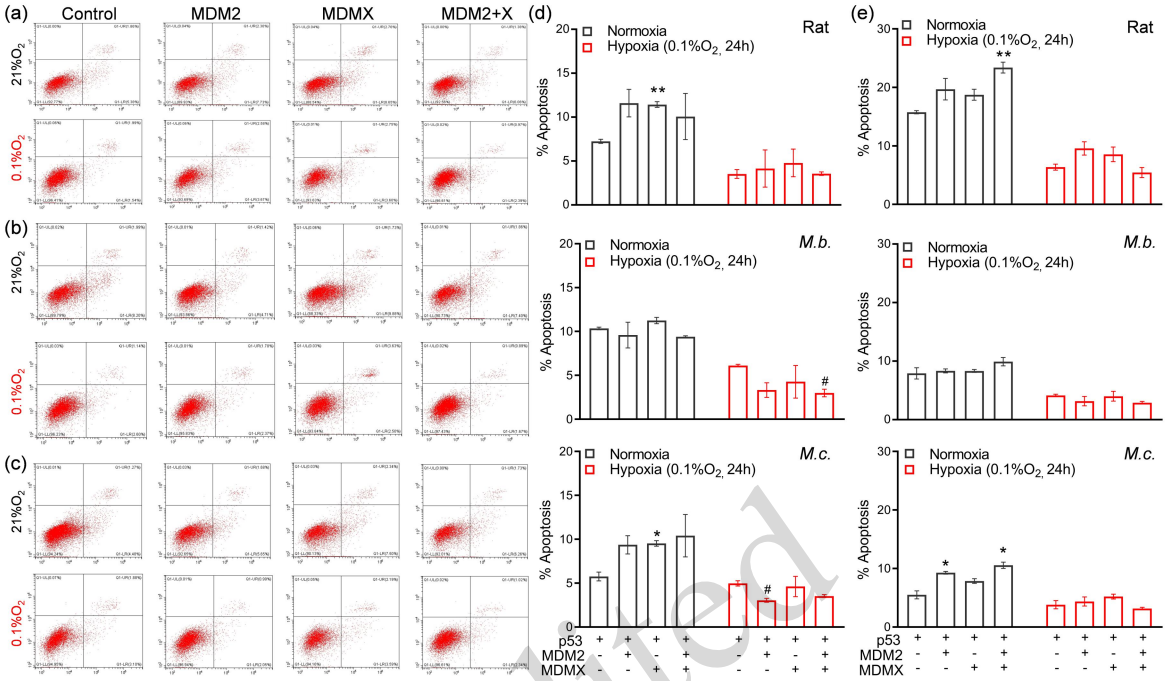

Fig. 4 MDM2/X mediated lower apoptosis in *M.b.* and *M.c.* under normoxia and hypoxia. Apoptosis induced by p53 (combined with MDM2 or MDMX) of lab rats (a), *M.b.* (b), and *M.c.* (c) in the H1299 cell line was determined by using flow cytometry. Summarized data in H1299 (d) and HEK293T (e) cell lines showed low levels of MDM2/MDMX-induced p53-dependent apoptosis in subterranean rodents. Values are given as mean±SEM, n=3, $^{*}P < 0.05$, $^{**}P < 0.01$ (*vs* normoxia trans-p53 only); $^{\#}P < 0.05$ (*vs* hypoxia trans-p53 only).

3.5 *M.b./M.c.*-MDM2 increases p53 mRNA and protein expression *via* C-terminal modifications

To investigate whether the decreased apoptosis of *M.b.* and *M.c.* under hypoxia is related to MDM2/X-mediated p53 expression, we overexpressed Rat-, *M.b.*-, and *M.c.*-p53, MDM2, and MDMX in the H1299 cells and tested p53 mRNA expression. Rat-MDMX and MDM2/X combination significantly decreased the p53 transcription under hypoxia, however, both *M.b.*- and *M.c.*-MDM2/X markedly increased p53 mRNA levels under hypoxia (Fig. 5a). Sequence alignment analysis found the critical substitutions in *M.b./M.c.*-MDM2 at two key phosphorylation sites: Y390F (c-Abl tyrosine kinase recognition site) and T415A (ATM serine/threonine kinase recognition site), which conserved as Y and T in humans and rats, respectively (Fig. 5b). Functional characterization of these variations through site-directed mutagenesis found that wild-type *M.b.*- and *M.c.*-MDM2 (wt-A415) enhanced p53 mRNA expression under hypoxia, while the mutant MDM2 (mut-T415, like humans) abolished this effect. Combined MDM2 with MDMX also potentiated p53 transcription, whereas mut-MDM2 (T415) with MDMX blocked the enhanced p53 mRNA expression (Fig. 5c). These findings identified that the variations of *M.b./M.c.*-MDM2 contribute to the accumulation of p53 transcription under hypoxia stress *via* C-terminal loss-of-phosphorylation modification, but the co-factor MDMX had little effect. Furthermore, we observed that transfected Rat-MDM2 can inhibit p53 protein expression in a dose-dependent manner of MDM2, reversible by Nutlin-3a (an inhibitor of the MDM2-p53 interaction by binding to the binding cleft of MDM2; Anil, et al., 2013). However, over-expressed *M.b.*-MDM2-wt (A415, F390) significantly increased p53 protein levels dose-dependently. Notably, reactivating the c-Abl and ATM kinase on MDM2 phosphorylation of *M.b.*, the mut-MDM2 (A415T and F390Y) blocked the elevated-p53 protein, depending on MDM2-doses (declining trend) (Fig. 5d), which indicated that wt-MDM2 of *M.b.* and *M.c.* (A415, F390) abolished the MDM2 canonical function on p53 suppression, leading to p53 accumulation both on mRNA and protein levels. In addition, we analyzed the predicted 3D structures of MDM2, MDM2-p53 complex, MDMX, and p53 proteins in rats, *M.b.*, and *M.c.*, respectively (Fig. S4 and S5).

The monomer structures of MDM2, MDMX, or p53 are similar in the functional domains of these species (Fig. S4a and S5). But, some disorder chains at the MDM2 C-terminus cause the mismatching structures in Rat and *M.b.* (Fig. S4b$_1$). The variations of F390 and A415 in *M.b.*-MDM2 modified the hydrogen bonds between residues (F390 gain and A415 loss) (Fig. S4b$_2$-b$_3$). The overall arrangements of the p53 monomer-MDM2 complex in rat and *M.b.* are highly similar to each other (Fig. S4c). We further analyzed the structures of the p53 dimer-MDM2 complex that initiates the p53 degradation *via* ubiquitination. In the Rat-p53 dimer-MDM2, the structures of the C-terminal portion of MDM2 adopt relatively stable helices in proximity to Rat-p53, whereas the C-terminal disordered chains of *M.b.*-MDM2 (near the F390 and A415 variations) were observed in the *M.b.*-p53 dimer-MDM2 complex, indicating its greater flexibility. These natural MDM2 variation sites lost the c-Abl/ATM-mediated phosphorylation, which might be beneficial for the adaptation to the underground conditions by mediating the low apoptosis depending on the stable-p53 (Fig. 5e).

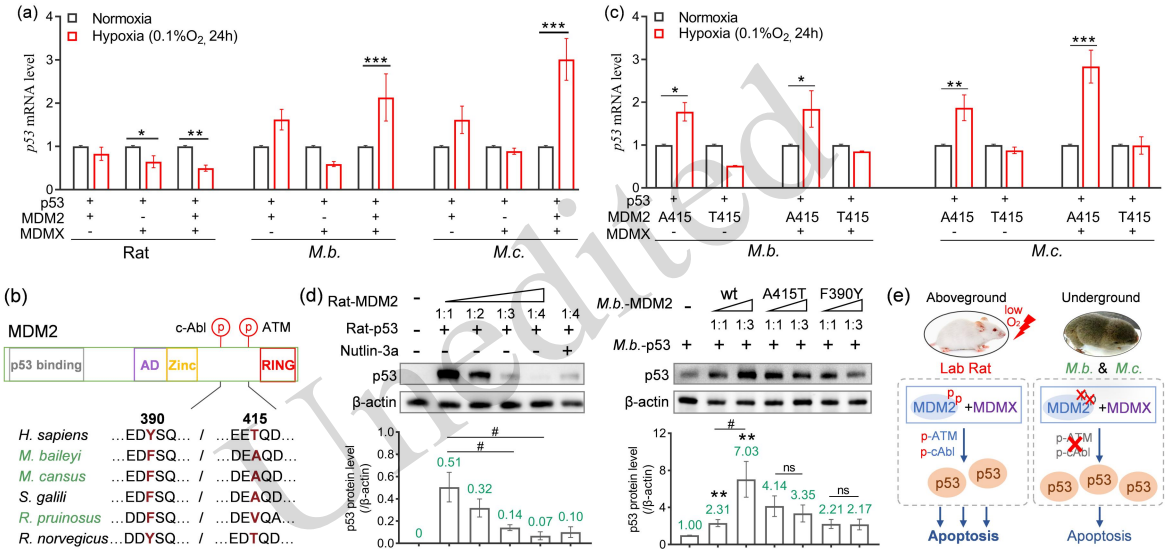

Fig. 5 *M.b.*/*M.c.*-MDM2/X involved in the upregulation of p53 mRNA and protein. (a) MDM2 and MDMX of *M.b.*/*M.c.* increased p53 mRNA expression under hypoxic stress. Values are given as mean±SEM, n=3, $^{*}P < 0.05$, $^{**}P < 0.01$, $^{***}P < 0.001$ (*vs* normoxia). (b) Diagram for the F390 and A415 variation sites in the C-terminal of MDM2 CDS sequences. (c) *M.b.*/*M.c.*-mut-MDM2 (T415) blocked hypoxia-enhanced p53 mRNA expression in the H1299 cell lines. Values are given as mean±SEM, n=3, $^{*}P < 0.05$, $^{**}P < 0.01$, $^{***}P < 0.001$ (*vs* normoxia). (d) Rat-MDM2 decreased p53 protein level in MDM2 doses-dependently, while *M.b.*-wt-MDM2 upregulated p53, but A415T and F390Y mutations of *M.b.*-MDM2 doses-dependently decreased p53 protein level. Values are given as mean±SEM, n=3, $^{*}P < 0.05$, $^{**}P < 0.01$ (*vs* trans-p53 only); $^{\#}P < 0.05$ (*vs* co-trans-p53:MDM2 wt=1:1). (e) Heterodimer MDM2/MDMX is activated under hypoxia in aboveground lab rats, increases p53 expression through ATM and c-Abl kinases (MDM2-T415/Y390), and causes p53-dependent apoptosis. While in subterranean zokors, the loss-of-phosphorylation variations (A415 and F390) inhibit the MDM2 activation, but still induce p53 accumulation (mRNA and protein) with low apoptosis.

4 Discussion

4.1 Evolution and diversity of MDM2/X variations

MDM genes are involved in the adaptations to stress and precise control over the tumor suppressor p53. Vertebrates carry both paralogues MDM2 and MDMX (Tan, et al., 2017). We found the evolutionary conservation of MDM2/X in both subterranean and aboveground species (Fig. 1a), such as *Spalacidae* (*M.b.*, *M.c.*, *N.g.*, and *R.p.*), *Hystricomorpha* (naked mole rat, Damaraland mole rat, and guinea pig), and *Insectivora* (star-nosed mole and shrew), indicating MDM family share a common ancestral gene; the duplication event

possibly occurred early in vertebrate evolution. Both MDM2 and MDMX have the p53-binding, Acidic, Zinc finger, and RING domains that are conserved throughout evolution (Fig. S1 and S2), which explains the variation sites of *M.b*., *M.c*., and *R.p*. mainly in non-domain regions (Fig. 1b). The p53-MDM2 interaction and MDM2/X E3 ligase activity existed in the common ancestor of vertebrates, lampreys (Coffill, et al., 2016; Levine, 2020), suggesting MDM2/X co-evolution with the p53 pathway and keeping a conserved cellular role throughout history. The overall homology of MDM2 and p53 among *Spalacidae* is higher than MDMX, and subterranean species are more conserved compared to the aboveground orthologs, implying the p53-MDM2 functions are preserved in underground environments.

As mentioned above, *M.b*. and *M.c*. live underground in the plateau, with extremely low oxygen and high carbon dioxide challenges for animal survival. We proposed wild *M.b*./*M.c*. exhibit an evolutionary trade-off: optimize for hypoxia tolerance *via* HIF-1α (Chen et al., 2007) and MDM2/X, whereas lab rats prioritize genome integrity (ATM/ATR-MDM2/X) at the expense of hypoxia resistance. Subterranean species generally showed enhanced hypoxia-related pathways, such as red blood cell function, blood vessel development, heart function, ATPase activity, and aerobic respiration (Deng et al., 2014; Shao et al., 2015; Hu et al., 2023). Notably, *M.b*. living at high altitudes have evolved more finely-tuned patterns of hypoxia adaptation, zokors from different elevations showed altitude-dependent gene transcriptional change and cardiac-blood phenotypes (Cai et al., 2018; Wei et al., 2025). However, as the same rodent family (*Spalacidae*) members, bamboo rats (*R.p.*) could represent an intermediate model for hypoxia adaptation. In contrast to high-altitude zokors (*M.b*./*M.c.*), which endure extreme hypoxia, *R.p*. inhabits subterranean burrows in tropical/subtropical regions with warmer, humid conditions and moderate oxygen limitation, while displaying greater stress resistance than aboveground rodents (Gao et al., 2023). *R.p*.-MDM2/X are convergent from *M.b*., *M.c*., and *N.g*., which supported that *Myospalacinae* (*M.b*./*M.c*. subfamily) and *Rhizomyinae* (*R.p*. subfamily) are sister relationships based on the genome analysis (Guo et al., 2021). Bamboo rats shared many convergent genes with Chinese zokors and Israeli blind mole rats compared with the aboveground controls; these genes were also enriched in the hypoxia-related pathways, such as response to oxidative stress, angiogenesis, and carboxylic acid transport (Ashur-Fabian et al., 2004; Gorbunova et al., 2012; Cao et al., 2020; Guo et al., 2021). However, *R.p*. exhibits distinct physiological traits due to its particular life habits and herbivorous diet in bamboo consumption; the larger body size than *M.b*., *M.c*., and *N.g*. requires higher metabolic demands but slower respiration rates (Xiao et al., 2022; Gan et al., 2023). Therefore, *R.p.* MDM2/X co-evolution with zokors, but introduces novel modifications, such as Valine (V) in MDM2-codon 415, which is a different variation but functions the same as alanine (A) in *M.b*., *M.c*., and *N.g*.. The life ecology of bamboo rats is more similar to that of Israeli *Spalax*, facing intermittent low oxygen stress, may show flexible p53 reactivation post-hypoxia, and rely less on HIF than *M.b*. Thus, the life-history traits of *M.b*., *M.c*., and *R.p*. shape the diverse evolutionary dynamics for the adaptations to the hypoxic underground environment.

4.2 MDM2-mediated p53 functions contribute to apoptosis

The transcription factor p53 has a central role in response to cellular stress. Activated p53 regulates hundreds of target genes to determine cell fates, including DNA damage response, cell cycle arrest, apoptosis, and senescence (Oren and Prives, 2024). In subterranean rodents, the different methylation levels of the *N.g*.-p53 promoters result in the differential expression of p53, which selectively changes the adaptive cell-cycle arrest (Zhao et al., 2016). Meanwhile, previously we found that *M.b*.-p53 has a special codon 104N variation near the TAD (transactivation domain), which is responsible for the transactivation of apoptotic genes under environmental stresses. *M.b*.-p53 reduced the apoptosis rate under hypoxia (0.2% O_2), cold (30 °C), and acidic stress (pH 6.6) by decreasing the mRNA expression of pro-apoptotic genes (*Bax*, *Puma*, and *Igfbp3*) transcriptions, and up-regulating *Bcl-2* levels (Zhao et al., 2013). We further observed that p53 and MDM2 exhibited high levels of transcription and protein expression in the lung and liver tissues of *M.b*. and *M.c*. (Fig. 2 and 3); and hypoxia induced p53 mRNA expression *via* both *M.b*./*M.c*.-MDM2 and MDM2/X heterodimer

(Fig. 5a). Therefore, the accumulated *M.b.*/*M.c.*-p53 contributes to the anti-apoptotic under hypoxic conditions. The high expressions of both p53 and MDM2 further supported that *M.b.*/*M.c.*-MDM2 is also recruited for hypoxia survival, and extreme underground environments stimulate *M.b.*/*M.c.* evolved under the favoring MDM2/X.

In *M.b.* and *M.c.*, MDM2 and MDMX demonstrated functional divergent yet cooperative roles in conferring hypoxia resistance. Single MDMX cannot show the same functions as MDM2; data related to MDMX mutations also failed to show the changes in p53 expression and apoptosis. However, the combination of MDM2/X increased p53 mRNA and enhanced the regulation of p53 functions. *M.b.*-MDM2+MDMX+p53 showed significantly reduced apoptosis under 0.1% hypoxic challenge, whereas *M.c.*-MDM2+p53 displayed a lower apoptosis rate. This suggested that evolutionary adaptations in wild animals under extreme environments could reveal mutation mechanisms to guide drug design, mimicking nature's million years of selection. Currently, MDM2 inhibitors, double MDM2+MDMX inhibitors, and MDM2 degraders (PROTACs) are being explored for therapeutic antitumor treatment or anti-inflammation (Fang et al., 2020; Zhang et al., 2023; Wang C et al., 2024; Wang W et al., 2024). However, challenges such as side effects, resistance, and toxicity persist in canonical conventional lab models (rats or mice) (Peuget et al., 2024; Tuval et al., 2024), and studying natural adaptations may offer strategies to refine these mechanisms.

The MDM2-MDMX-p53 axis exhibits striking functional differences between subterranean rodents (*M.b.*, *M.c.*) and lab rats, reflecting their distinct evolutionary pressures and physiological demands. In addition, p53 dynamically regulates the balance between cell apoptosis and survival through MDM2 and MDMX. Wild *M.b.*/*M.c.* maintain a well-balanced equilibrium, characterized by a higher apoptosis threshold, which confers resistance to hypoxia-induced cell death; lab rats, on the other hand, exhibit a lower apoptosis threshold, making them sensitive to DNA damage but robustly maintaining genome integrity.

4.3 MDM2 mutations at phosphorylation sites involved in p53 functions

Posttranslational modification plays an important role in the MDM2/X-p53 regulation. ATM (Ataxia Telangiectasia Mutated), c-Abl (ABL1), and Chk1/2 (Checkpoint Kinase 1/2) are critical kinases that regulate the phosphorylation of MDM2, MDMX, and p53 in response to DNA damage and hypoxia stress (Goldberg et al., 2002; Chen et al., 2005; Gajjar et al., 2012; Olcina et al., 2014; Carr et al., 2016; Hashimoto et al., 2018; Shi et al., 2020). The classical phospho-sites, such as Hu-p53 Ser15, Hu-MDMX Ser403, and Hu-MDM2 Ser395 in humans, were highly conserved across species, including *M.b.* and *M.c.* (Fig. S1-S3). However, we found two specific variations (F390 and A415) on the ATM/c-Abl-targeted phospho-sites in *M.b.*/*M.c.*-MDM2, which might influence p53 stability and cell outcome decisions (Cheng et al., 2009; Cheng et al., 2011; Karakostis et al., 2024).

Following stress, ATM phosphorylates MDM2 on six sites (Hu-MDM2-Ser386, Ser395, Ser407, Thr419, Ser425, and Ser429) between the Acidic/Zinc domain and RING domains (Gannon et al., 2012); and c-Abl activates Hu-MDM2-Tyr394 (Y394) (Goldberg et al., 2002, and Carr et al., 2016). The target of MDM2 ubiquitination degradation was changed from p53 to MDM2/X heterodimer itself, which significantly disrupts p53 degradation and guides the stable p53 facing stress (Cheng et al., 2011; Pant and Lozano, 2014; Carr et al., 2016; Medina et al., 2016; Wu et al., 2024). We surprisingly found that MDM2 variation sites, F390 and A/V415 (corresponding to Y and T in humans and rats), lost phosphorylation in the *Spalacidae* family species from China to Israel (*M.b.*, *M.c.*, *N.g.*, and *R.p.*). The codon 415 in *M.b.*, *M.c.*, and *N.g.* is the same alanine (A, a classical substitution for non-phosphorylation), while *R.p.* evolved a novel mutation (Valine, V), which is electrically neutral at physiological pH, and also fails to be phosphorylated like alanine. *M.b.*-MDM2 wt-A415 lose the hydrogen bond with E414 (corresponding to Rat-MDM2 D414 and Hu-MDM2 E418), however, the hydrogen bond exists between Rat-MDM2 D414-T415 (Hu-MDM2 E418-T419) (Fig. S4b$_3$). Meanwhile, the F390 variation is the same Phenylalanine in *M.b.*, *M.c.*, *N.g.*, and *R.p.* from the *Spalacidae* family. *M.b.*-MDM2 wt-F390 adopt a hydrogen bond with S391 (Rat-MDM2 S391 and Hu-MDM2 S395: the ATM classical

phospho-site), which is not between Rat-MDM2 Y390-S391 (Hu-MDM2 Y394-S395) (Fig. S4b$_2$). These changes in the hydrogen bonds may decrease the structural stability and disrupt the native conformations.

The disordered chains exist in a collection of dynamic interconverting conformations with unstable 3D structure; it is essential for transcriptional control, cell signaling, and subcellular organization (Holehouse and Kragelund, 2024). MDM2 degraded p53 by closely binding to the p53 dimer. The F390 and A415 in this disorder chain led to the different MDM2 conformations between *M.b*. and Rat (Fig. S4b$_1$), and the unstable C-terminal portion of MDM2 in *M.b*.-p53 dimer-MDM2 complex (Fig. S4c). The sequences and structures of the classical N-terminal p53-MDM2 interaction region (p53 transactivation domain, including BOX-I motif) are conserved in rat, *M.b*., and *M.c*. (Fig. S3 and S5a) (Padariya et al., 2022). Therefore, *M.b*.-MDM2 F390 and A415 in the C-terminal disordered chain might blunt the p53 ubiquitination.

In humans, Hu-MDM2-Y394 and T419 (*M.b*.-MDM2 F390 and A415) are redundant in MDM2-p53 signaling by ATM-Abl phosphorylation (Goldberg et al., 2002; Cheng et al., 2009; Cheng et al., 2011; Carr et al., 2016). However, our findings supported that the natural *M.b*./*M.c*.-MDM2 F390/A415 increased the p53 expression in mRNA and protein levels; the artificial mutations (F390Y and A415T) restored phosphorylation but blocked the p53 accumulation in zokors. These results suggest that it is the *M.b*./*M.c*.-MDM2 variations that disrupted the ATM/c-Abl-mediated phosphorylation under subterranean environments, which elicited a specific dynamic balance of p53 accumulation and apoptosis suppression in zokors. Therefore, subterranean species evolved the uniquely adaptable p53-MDM2/X axis to favor cell survival.

5 Conclusions

The MDM2-MDMX-p53 in wild subterranean rodents exemplifies evolutionary innovation under extreme environments, while lab rats preserve ancestral mammalian regulation. The evolution of *Mdm2*, *Mdmx*, and *p53* genes, with their special regulation loop, mediates the underground and aboveground species in different paths, but leads to the same survival under stress. These natural evolutions of molecular mechanisms highlight how gene networks can be repurposed when survival trumps tumor suppression. It is important for evolutionary biology, stress adaptation, and medicine.

Data availability statement

All data supporting the findings of this study are contained within the paper and its supplementary materials.

Acknowledgments

This work is supported by grants from the National Natural Science Foundation of China (Xuequn CHEN: 32120103007, 81930054; Yang ZHAO: 32371236), the National Key Basic Research Programs of China (973 project, Jizeng DU: 2012CB518200), and Ancell-Teicher Research Foundation for Genetics and Molecular Evolution (Eviatar NEVO). The authors are grateful for the technical support of the Core Facilities, Zhejiang University School of Medicine.

Author contributions

Xuequn CHEN, Yang ZHAO, and Jizeng DU designed the research and supervised the study. Mengchen ZHANG, Eviatar NEVO, Yang ZHAO, and Xuequn CHEN wrote the manuscript. Mengchen ZHANG and Yi LI performed molecular and cellular experiments and statistical analysis. Huiqi LIN and Fangyuan XIA contribute to genetic evolution analysis. Tianfu YU, Chatoo MAHANAND, Kexin LI, Honghao YU, Yang ZHAO, Eviatar NEVO, and Xuequn CHEN collected *N.g*., *M.b*., *M.c*., and *R.p*. animal samples. All authors have read and approved the final manuscript, and therefore, have full access to all the data in the study and take responsibility for the integrity and security of the data.

Compliance with ethics guidelines

Mengchen ZHANG, Yi LI, Huiqi LIN, Tianfu YU, Fangyuan XIA, Chatoo MAHANAND, Kexin LI, Honghao YU, Eviatar

NEVO, Jizeng DU, Yang ZHAO, and Xuequn CHEN declare that they have no conflict of interest.

All experiments were performed under the Guide for the Care and Use of Laboratory Animals, and approved by the Laboratory Animal Welfare and Ethics Committee of Zhejiang University, Hangzhou, China (Certificate No. ZJU20220102).

References

An X, Mao LY, Wang YJ, et al., 2024. Genomic structural variation is associated with hypoxia adaptation in high-altitude zokors. *Nat Ecol Evol*, 8(2):339–351.
https://doi.org/10.1038/s41559-023-02275-7

Anil B, Riedinger C, Endicott JA, et al., 2013. The structure of an MDM2-Nutlin-3a complex solved by the use of a validated MDM2 surface-entropy reduction mutant. *Acta Crystallogr D Biol Crystallogr*, 69(Pt 8):1358-1366.
https://doi:10.1107/S0907444913004459

Ashur-Fabian O, Avivi A, Trakhtenbrot L, et al., 2004. Evolution of p53 in hypoxia-stressed Spalax mimics human tumor mutation. *Proc Natl Acad Sci U S A*, 101(33):12236–12241.
https://doi.org/10.1073/pnas.0404998101

Brummer T, Zeiser R, 2024. The role of the MDM2/p53 axis in antitumor immune responses. *Blood*, 143(26):2701–2709.
https://doi.org/10.1182/blood.2023020731

Cai ZY, Wang LY, Song XY, et al., 2018. Adaptive transcriptome profiling of subterranean zokor, Myospalax baileyi, to high-altitude stresses in Tibet. *Sci Rep*, 8(1):4671.
https://doi.org/10.1038/s41598-018-22483-7

Cao WJ, Pu P, Wang JZ, et al., 2020. Suppressed LPS-mediated TLR4 signaling in the plateau zokor (Eospalax baileyi) compared to the bamboo rat (Rhizomys pruinosus) and rat (Rattus norvegicus). *J Exp Zool Ecol Integr Physiol*, 333(4):240–251.
https://doi.org/10.1002/jez.2346

Carr MI, Roderick JE, Zhang H, et al., 2016. Phosphorylation of the Mdm2 oncoprotein by the c-Abl tyrosine kinase regulates p53 tumor suppression and the radiosensitivity of mice. *Proc Natl Acad Sci U S A*, 113(52):15024–15029.
https://doi.org/10.1073/pnas.1611798114

Chandramohan A, Josien H, Yuen TY, et al., 2024. Design-rules for stapled peptides with in vivo activity and their application to Mdm2/X antagonists. *Nat Commun*, 15(1):489.
https://doi.org/10.1038/s41467-023-43346-4

Chen L, Gilkes DM, Pan Y, et al., 2005. ATM and Chk2-dependent phosphorylation of MDMX contribute to p53 activation after DNA damage. *EMBO J*, 24(19):3411-3422.
https://doi.org/10.1038/sj.emboj.7600812

Chen XQ, Wang SJ, Du JZ, et al., 2007. Diversities in hepatic HIF-1, IGF-I/IGFBP-1, LDH/ICD, and their mRNA expressions induced by CoCl(2) in Qinghai-Tibetan plateau mammals and sea level mice. *Am J Physiol Regul Integr Comp Physiol*, 292(1):R516–R526.
https://doi.org/10.1152/ajpregu.00397.2006

Cheng Q, Chen L, Li Z, et al., 2009. ATM activates p53 by regulating MDM2 oligomerization and E3 processivity. *EMBO J*, 28(24):3857–3867.
https://doi.org/10.1038/emboj.2009.294

Cheng Q, Cross B, Li BZ, et al., 2011. Regulation of MDM2 E3 ligase activity by phosphorylation after DNA damage. *Mol Cell Biol*, 31(24):4951–4963.
https://doi.org/10.1128/MCB.05553-11

Chibaya L, Karim B, Zhang H, et al., 2021. Mdm2 phosphorylation by Akt regulates the p53 response to oxidative stress to promote cell proliferation and tumorigenesis. *Proc Natl Acad Sci U S A*, 118(4):e2003193118.
https://doi.org/10.1073/pnas.2003193118

Coffill CR, Lee AP, Siau JW, et al., 2016. The p53-Mdm2 interaction and the E3 ligase activity of Mdm2/Mdm4 are conserved from lampreys to humans. *Genes Dev*, 30(3):281–292.
https://doi.org/10.1101/gad.274118.115

Corpet F, 1988. Multiple sequence alignment with hierarchical clustering. *Nucleic Acids Res*, 16(22):10881–10890.
https://doi.org/10.1093/nar/16.22.10881

Deng XG., Wang K, Zhang SD, et al., 2014. Transcriptomatic determination of convergent evolution between plateau zokors (Eospalax baileyi) and naked mole rats (Heterocephalus glaber). *Acta Theriol Sin*, 34(2):129–137. (in Chinese)

Efe G, Rustgi AK, Prives C, 2024. p53 at the crossroads of tumor immunity. *Nat Cancer*, 5(7):983–995.
https://doi.org/10.1038/s43018-024-00796-z

Fang Y, Liao G, Yu B, 2020. Small-molecule MDM2/X inhibitors and PROTAC degraders for cancer therapy: advances and perspectives. *Acta Pharm Sin B*, 10(7):1253–1278.
https://doi.org/10.1016/j.apsb.2020.01.003

Gajjar M, Candeias MM, Malbert-Colas L, et al., 2012. The p53 mRNA-Mdm2 interaction controls Mdm2 nuclear trafficking and is required for p53 activation following DNA damage. *Cancer Cell*, 21(1):25-35. https://doi.org/10.1016/j.ccr.2011.11.016

Gan Y, Wu YJ, Dong YQ, et al., 2023. The study on the impact of sex on the structure of gut microbiota of bamboo rats in China. *Front Microbiol*, 14:1276620. https://doi.org/10.3389/fmicb.2023.1276620

Gannon HS, Woda BA, Jones SN, 2012. ATM phosphorylation of Mdm2 Ser394 regulates the amplitude and duration of the DNA damage response in mice. *Cancer Cell*, 21(5):668–679. https://doi.org/10.1016/j.ccr.2012.04.011

Gao CH, Li JM, Xu B, et al., 2023. Responses of blood parameters and hemoglobin subtypes in plateau zokors and plateau pikas to different altitude habitats. *Acta Physiol Sin*, 75(1):69–81. (in Chinese)

Goldberg Z, Vogt Sionov R, Berger M, et al., 2002. Tyrosine phosphorylation of Mdm2 by c-Abl: implications for p53 regulation. *EMBO J*, 21(14):3715–3727. https://doi.org/10.1093/emboj/cdf384

Gorbunova V, Hine C, Tian X, et al., 2012. Cancer resistance in the blind mole rat is mediated by concerted necrotic cell death mechanism. *Proc Natl Acad Sci U S A*, 109(47):19392–19396. https://doi.org/10.1073/pnas.1217211109

Guo YT, Zhang J, Xu DM, et al., 2021. Phylogenomic relationships and molecular convergences to subterranean life in rodent family Spalacidae. *Zool Res*, 42(5):671–674. https://doi.org/10.24272/j.issn.2095-8137.2021.240

Hashimoto T, Murata Y, Urushihara Y, et al, 2018. Severe hypoxia increases expression of ATM and DNA-PKcs and it increases their activities through Src and AMPK signaling pathways. *Biochem Biophys Res Commun*, 505(1):13–19. https://doi.org/10.1016/j.bbrc.2018.09.068

Holehouse AS, Kragelund BB, 2024. The molecular basis for cellular function of intrinsically disordered protein regions. *Nat Rev Mol Cell Biol*, 25(3):187-211. https://doi:10.1038/s41580-023-00673-0

Hu YB, Wang XP, Xu YC, et al., 2023. Molecular mechanisms of adaptive evolution in wild animals and plants. *Sci China Life Sci*, 66(3):453–495. https://doi.org/10.1007/s11427-022-2233-x

Karakostis K, Malbert-Colas L, Thermou A, et al., 2024. The DNA damage sensor ATM kinase interacts with the p53 mRNA and guides the DNA damage response pathway. *Mol Cancer*, 23(1):21. https://doi.org/10.1186/s12943-024-01933-z

Levine AJ, 2020. p53: 800 million years of evolution and 40 years of discovery. *Nat Rev Cancer*, 20(8):471–480. https://doi.org/10.1038/s41568-020-0262-1

Liu X, Zhang SZ, Cai ZY, et al., 2022. Genomic insights into zokors' phylogeny and speciation in China. *Proc Natl Acad Sci U S A*, 119(19):e2121819119. https://doi.org/10.1073/pnas.2121819119

Medina-Medina I, García-Beltrán P, de la Mora-de la Mora I, et al., 2016. Allosteric interactions by p53 mRNA govern HDM2 E3 ubiquitin ligase specificity under different conditions. *Mol Cell Biol*, 36(16):2195–2205. https://doi.org/10.1128/MCB.00113-16

Olcina MM, Grand RJ, Hammond EM, 2014. ATM activation in hypoxia-causes and consequences. *Mol Cell Oncol*, 1(1):e29903. https://doi.org/10.4161/mco.29903

Oren M, Prives C, 2024. p53: A tale of complexity and context. *Cell*, 187(7):1569–1573. https://doi.org/10.1016/j.cell.2024.02.043

Padariya M, Jooste ML, Hupp T, et al., 2022. The elephant evolved p53 isoforms that escape MDM2-mediated repression and cancer. *Mol Biol Evol*, 39(7):msac149. https://doi:10.1093/molbev/msac149

Pant V, Lozano G, 2014. Limiting the power of p53 through the ubiquitin proteasome pathway. *Genes Dev*, 28(16):1739-1751. https://doi.org/10.1101/gad.247452.114

Peuget S, Zhou XL, Selivanova G, 2024. Translating p53-based therapies for cancer into the clinic. *Nat Rev Cancer*, 24(3):192–215. https://doi.org/10.1038/s41568-023-00658-3

Shao Y, Li JX, Ge RL, et al., 2015. Genetic adaptations of the plateau zokor in high-elevation burrows. *Sci Rep*, 5:17262 https://doi.org/10.1038/srep17262

Shi Y, Liu Z, Zhang Q, et al., 2020. Phosphorylation of seryl-tRNA synthetase by ATM/ATR is essential for hypoxia-induced angiogenesis. *PLoS Biol*, 18(12):e3000991.

https://doi.org/10.1371/journal.pbio.3000991
Tan BX, Liew HP, Chua JS, et al., 2017. Anatomy of Mdm2 and Mdm4 in evolution. *J Mol Cell Biol*, 9(1):3–15. https://doi.org/10.1093/jmcb/mjx002
Tian Y, Niu Y, Ji C, et al., 2017. A study of the gas environment in foraging tunnels of plateau zokor (Myospalax baileyi) in the eastern Qilian Mountain region. *Acta Theriologica Sinica*, 37(2):152-161. https://doi:10.16829/j.slxb.201702006
Tuval A, Strandgren C, Heldin A, et al., 2024. Pharmacological reactivation of p53 in the era of precision anticancer medicine. *Nat Rev Clin Oncol*, 21(2):106–120. https://doi.org/10.1038/s41571-023-00842-2
Wang C, Zhang YJ, Chen WJ, et al., 2024. New-generation advanced PROTACs as potential therapeutic agents in cancer therapy. *Mol Cancer*, 23(1):110. https://doi.org/10.1186/s12943-024-02024-9
Wang W, Albadari N, Du Y, et al., 2024. MDM2 inhibitors for cancer therapy: the past, present, and future. *Pharmacol Rev*, 76(3):414–453. https://doi.org/10.1124/pharmrev.123.001026
Wei DB, Wei L, Zhang JM, et al., 2006. Blood-gas properties of plateau zokor (Myospalax baileyi). *Comp Biochem Physiol A Mol Integr Physiol*, 145(3):372–375. https://doi.org/10.1016/j.cbpa.2006.07.011
Wei YY, Zhang T, Li ZF, et al., 2025. Evolutionary divergence on the Qinghai-Tibet Plateau: How life-history traits shape the diversity of plateau zokor and pika populations. *J Genet Genomics*, S1673-8527(25)00128-6. https://doi.org/10.1016/j.jgg.2025.04.019
Wu KL, Xu XF, Wu MY, et al., 2024. MDM2 induces pro-inflammatory and glycolytic responses in M1 macrophages by integrating iNOS-nitric oxide and HIF-1α pathways in mice. *Nat Commun*, 15(1):8624. https://doi.org/10.1038/s41467-024-53006-w
Xiao KP, Liang XH, Lu HR, et al., 2022. Adaptation of gut microbiome and host metabolic systems to lignocellulosic degradation in bamboo rats. *ISME J*, 16(8):1980–1992. https://doi.org/10.1038/s41396-022-01247-2
Yu ZQ, Zhang EE. 2023. Disrupted circadian rhythms in the plateau pika. *Trends Neurosci*, 46(12):1005–1007. https://doi.org/10.1016/j.tins.2023.09.003
Zeng J, Wang Z, Shi Z, 1984. Metabolic characteristics and some physiological parameters of mole rat (Myospalax baileyi) in alpine area. *Acta Biol Plateau Sin*, 3:163-171. (in Chinese)
Zhang ST, Zhao Y, Hu XF, et al., 2013. Distinct post-transcriptional regulation of Igfbp1 gene by hypoxia in lowland mouse and Qinghai-Tibet plateau root vole Microtus oeconomus. *Mol Cell Endocrinol*, 376(1-2):33–42. https://doi.org/10.1016/j.mce.2013.05.025
Zhang T, Lei ML, Zhou H, et al., 2022. Phylogenetic relationships of the zokor genus Eospalax (Mammalia, Rodentia, Spalacidae) inferred from whole-genome analyses, with description of a new species endemic to Hengduan Mountains. *Zool Res*, 43(3):331–342. https://doi.org/10.24272/j.issn.2095-8137.2022.045
Zhang NY, Hou DY, Hu XJ, et al., 2023. Nano proteolysis targeting chimeras (PROTACs) with anti-hook effect for tumor therapy. *Angew Chem Int Ed Engl*, 62(37):e202308049. https://doi.org/10.1002/anie.202308049
Zhang XY, Khakisahneh S, Liu W, et al., 2023. Phylogenetic signal in gut microbial community rather than in rodent metabolic traits. *Natl Sci Rev*, 10(10):nwad209. https://doi.org/10.1093/nsr/nwad209
Zhao Y, Ren JL, Wang MY, et al., 2013. Codon 104 variation of p53 gene provides adaptive apoptotic responses to extreme environments in mammals of the Tibet plateau. *Proc Natl Acad Sci U S A*, 110(51):20639–20644. https://doi.org/10.1073/pnas.1320369110
Zhao Y, Tang JW, Yang Z, et al., 2016. Adaptive methylation regulation of p53 pathway in sympatric speciation of blind mole rats, Spalax. *Proc Natl Acad Sci U S A*, 113(8):2146–2151. https://doi.org/10.1073/pnas.1522658112
Zhao Y, Zheng ZZ, Zhang ZH, et al., 2023. Evolution of high-molecular-mass hyaluronic acid is associated with subterranean lifestyle. *Nat Commun*, 14(1):8054. https://doi.org/10.1038/s41467-023-43623-2

Supplementary information

Table S1; Figs. S1-S5